Optical and ODMR Studies of Luminescent Halo(dimethylphenylphosphine)gold(I) Crystals

Brian Weissbart, Dawn V. Toronto, Alan L. Balch,* and Dino S. Tinti*

Department of Chemistry, University of California, Davis, California 95616

Received August 23, 1995[⊗]

Crystals of $\{(Me_2PhP)AuX\}_n$ (Me = methyl; Ph = phenyl; X = Cl, Br, I; n = 2, 3) show emission from two excited states. Both states are assigned a triplet multiplicity, on the basis of their lifetimes and zero-field splittings. The structured, higher energy emission originates at ≈360 nm and has the greater relative intensity at low temperatures. It is assigned as intraligand phosphorescence from a phenyl-localized $^3\pi\pi^*$ state. The unstructured, lower energy emission has a peak wavelength that varies in the range 630−730 nm. It is assigned as phosphorescence from the triplet state due to the gold-based $\sigma(p) \leftarrow \sigma^*(s,d)$ excitation. The corresponding singlet state is observed at 290−310 nm. The results of SCF−Xα−SW calculations on the model complexes H_3PAuX and $(H_3PAuX)_2$ are also presented.

Introduction

Luminescence has been reported from many mono- and multinuclear complexes of Au(I) with phosphine and related ligands.[1−8] The assignments of the luminescences have included excitations that involve metal and/or ligand orbitals. Many of the conclusions, however, are based on limited evidence, and the photophysics of the complexes remain poorly understood. We have recently shown that neat crystals of the monomeric complexes $(Ph_3E)AuX$ (Ph = phenyl; E = P, As; X = Cl, Br) exhibit two emission systems.[9] The systems have very similar properties among the four complexes. The higher energy system, which has its origin at ≈360 nm, was assigned as intraligand phosphorescence from a phenyl-localized $^3\pi\pi^*$ state of $(Ph_3E)AuX$. This was based on the vibronic analysis of the emission and the energy, lifetime, and zero-field splittings of the excited state. Perturbations in the properties of the $^3\pi\pi^*$ state appeared to be due to spin−orbit interactions with the gold center. The lower energy system has its origin at ≈450 nm. It also involves phosphorescence, on the basis of the lifetime and zero-field splittings of the excited state. However, the center or species responsible for the lower energy emission and its orbital assignment were unclear.

The present work investigates the luminescence of neat crystals of $(Me_2PhP)AuX$ (Me = methyl; X = Cl, Br, I). These crystals contain dimeric, $\{(Me_2PhP)AuX\}_2$ (X = Cl, Br, I), or trimeric, $\{(Me_2PhP)AuCl\}_3$, units with significant aurophilic attractions, as reported in the companion paper which gives the details of the crystal structures.[10] Crystals of $\{(Me_2PhP)AuX\}_n$ again show two emission systems. Emission, photoexcitation, absorption, and zero-field optically detected magnetic resonance (ODMR) spectra of the complexes and the kinetic parameters of the emissive excited states are reported and analyzed. The higher energy emission strongly resembles that of the corresponding system in $(Ph_3E)AuX$, but the lower energy emissions in the two groups of compounds are distinctly different. The results of SCF−Xα−SW calculations on H_3PAuX and $(H_3PAuX)_2$ are also presented to model the aurophilic interactions in the studied crystals.

Experimental Section

The compounds $\{(Me_2PhP)AuX\}_n$ were synthesized and purified as described in the companion paper.[10] Neat samples for spectroscopic study were single crystals or several small crystallites chosen from the purified materials. The results for $\{(Me_2PhP)AuCl\}_3$ are limited by the availability of crystals.

The instrumentation used to obtain the optical and ODMR spectra has been described earlier.[9] In brief, emission was excited with a filtered 100 W Hg or 75 W Xe lamp and recorded using a 1 m Czerny-Turner spectrometer. Photoexcitation studies used the Xe lamp with a 0.25 m monochromator for excitation, while detecting the emission with the 1 m spectrometer. All reported optical spectra are uncorrected for spectrometer sensitivity or lamp output. Measurements of the emission decay used a N_2 laser (337 nm) for pulsed excitation and, for lifetimes ≥1 ms, a mechanical shutter to extinguish the excitation from the Hg or Xe lamp. The decay data were accumulated using an averager and subsequently analyzed on a microcomputer with a least-squares algorithm. Raman spectra were obtained on polycrystalline samples (coarsely ground crystals) at 77 K using 488 nm radiation from an argon ion laser and a Spec Ramalab spectrometer.

[⊗] Abstract published in *Advance ACS Abstracts,* April 1, 1996.

(1) Ziolo, R. F.; Lipton, S.; Dori, Z. *J. Chem. Soc., Chem. Commun*. **1970**, 1124.
(2) King, C.; Wang, J.-C.; Khan, Md. N. I.; Fackler, J. P., Jr. *Inorg. Chem*. **1989**, *28*, 2145.
(3) King, C.; Khan, Md. N. I.; Staples, R. J.; Fackler, J. P., Jr. *Inorg. Chem*. **1992**, *31*, 3236. Assefa, Z.; Staples, R. J.; Fackler, J. P., Jr. *Inorg. Chem*. **1994**, *33*, 2790.
(4) (a) Assefa, Z.; McBurnett, B. G.; Staples, R. J.; Fackler, J. P., Jr.; Assmann, B.; Angermaier, K.; Schmidbaur, H. *Inorg. Chem*. **1995**, *34*, 75. (b) Assefa, Z.; McBurnett, B. G.; Staples, R.J.; Fackler, J. P., Jr. *Inorg. Chem*. **1995**, *34*, 4965.
(5) Markert, J. T.; Blom, N.; Roper, G.; Perregaux, A. D.; Nagasundaram, N.; Corson, M. R.; Ludi, A.; Nagle, J. K.; Patterson, H. H. *Chem. Phys. Lett*. **1985**, *118*, 258. Nagasundaram, N.; Roper, G.; Biscoe, J.; Chai, J. W.; Patterson, H. H.; Blom, N.; Ludi, A. *Inorg. Chem*. **1986**, *25*, 2947. Lacasce, J. H., Jr.; Turner, W. A.; Corson, M. R.; Dolan, P. J., Jr.; Nagle, J. K. *Chem. Phys*. **1987**, *118*, 289. Jones, W. B.; Yuan, J.; Narayanaswamy, R.; Young, M. A.; Elder, R. C.; Bruce, A. E.; Bruce, M. R. M. *Inorg. Chem*. **1995**, *34*, 1996.
(6) Parks, J. E.; Balch, A. L. *J. Organomet. Chem*. **1974**, *71*, 453. Balch, A. L.; Doonan, D. *J. Organomet. Chem*. **1977**, *131*, 137. Balch, A. L.; Catalano, V. J.; Olmstead, M. M. *Inorg. Chem*. **1990**, *29*, 585. Balch, A. L.; Fung, E. Y.; Olmstead, M. M. *Inorg. Chem*. **1990**, *29*, 3203. Toronto, D. V.; Balch, A. L.; Tinti, D. S. *Inorg. Chem*. **1994**, *33*, 2507.
(7) Che, C.-M.; Kwong, H.-L.; Yam, V. W.-W.; Cho, K.-C. *J. Chem. Soc., Chem. Commun*. **1989**, *885*. Che, C.-M.; Wong, W.-T.; Lai, T.-F.; Kwong, H.-L. *J. Chem. Soc., Chem. Commun*. **1989**, 243. Yam, W. V.-W.; Lai, T.-F.; Che, C.-M. *J. Chem. Soc., Dalton Trans*. **1990**, *11*, 3747. Che, C.-M.; Yap, H.-K.; Li, D.-M.; Pzng, S.-M.; Lee, G.-S.; Wang, Y.-M.; Liu, S.-T. *J. Chem. Soc., Chem. Commun*. **1991**, 1615.
(8) McClesky, T. M.; Gray, H. B. *Inorg. Chem*. **1992**, *31*, 1733.
(9) Larson, L. J.; McCauley, E. M.; Weissbart, B.; Tinti, D. S. *J. Phys. Chem*. **1995**, *99*, 7218.
(10) Toronto, D. V.; Weissbart, B.; Tinti, D. S.; Balch, A. L. *Inorg. Chem*. **1996**, *35*, 2484.

0020-1669/96/1335-2490$12.00/0

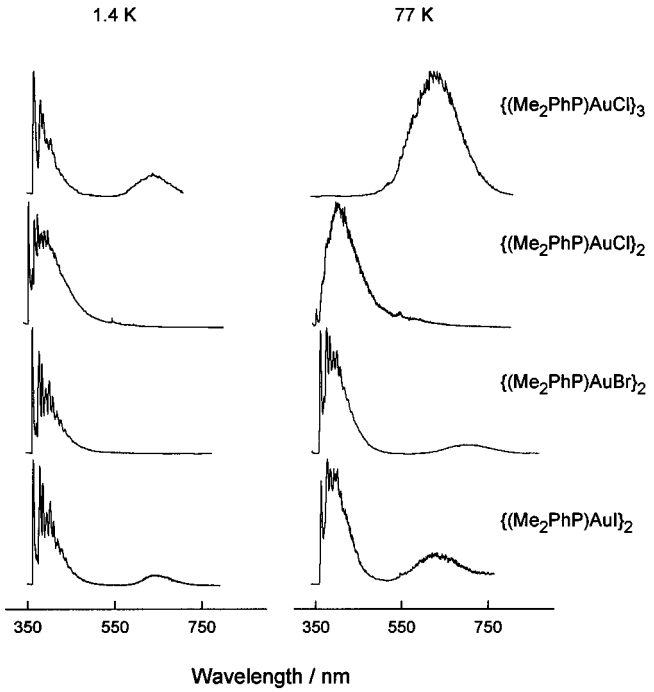

Figure 1. Survey emission spectra of crystalline $\{(Me_2PhP)AuX\}_n$ at 77 and 1.4 K, excited at 313 nm.

For the ODMR studies, the samples were at 1.4 K and in zero applied magnetic field. Excitation was provided by the filtered Hg lamp, and the emission intensity was monitored with the 1 m spectrometer at selected wavelengths. Slow-passage spectra were obtained using either amplitude-modulated microwave power with synchronous detection of the emission intensity in a single sweep or CW microwave power with summation of the dc signal from multiple sweeps in an averager. Transient ODMR signals for kinetic measurements were collected and analyzed analogously to optical decay data.

Standard SCF−Xα−SW calculations[11,12] were done on H_3PAuX and $(H_3PAuX)_2$ in C_{3v} and C_2 (perpendicular) point groups, respectively, for X = Cl, Br, and I. The Au−X and Au−P bond lengths were taken from known structures.[10,13,14] The P−H length was 1.40 Å, while the H−P−H angles were 95°. The Au−Au bond length was taken as 3.00 Å in the dimers, roughly 0.1−0.2 Å shorter than the experimental values in $\{(Me_2PhP)AuX\}_2$.[10] Other details were identical to those of earlier, related calculations.[9]

Results

Optical Spectra. Overviews of the emission spectra of neat crystals of $\{(Me_2PhP)AuX\}_n$ at 77 and 1.4 K for excitation at 313 nm are shown in Figure 1. All of the compounds show a structured emission system originating at ≈360 nm, and all except $\{(Me_2PhP)AuCl\}_2$ show a second unstructured system peaking in the range 630−730 nm. The luminescence spectrum of $\{(Me_2PhP)AuCl\}_2$ shows some variability among multiple samples, most notably in the weak structured emission at ≈540 nm and the apparent extra intensity around 400 nm. The latter are ascribed to an unknown impurity and/or trap. We will refer to the 360 and 630−730 nm systems as the HE (high-energy) and LE (low-energy) emissions, respectively. Table 1 summarizes the low-resolution origins of the HE emissions and the intensity maxima of the LE emissions.

Table 1. Summary of the Emission and Excitation Origins (HE) or Maxima (LE) for Crystalline $\{(Me_2PhP)AuX\}_n$ at 1.4 K

compound	emission/nm	excitation/nm
$\{(Me_2PhP)AuCl\}_2$	351	348
$\{(Me_2PhP)AuBr\}_2$	360	358
	720	≈300
$\{(Me_2PhP)AuI\}_2$	361	359
	645	309
$\{(Me_2PhP)AuCl\}_3$	361	358
	635	297

Table 2. Partial Vibronic Analysis of the HE Emission of Crystalline $\{(Me_2PhP)AuCl\}_2$ at 1.4 K

λ_{air}/nm	rel int[a]	ν_{vac}/cm^{-1}	$\Delta\nu$/cm^{-1}	assignment[b]
351.41	s	28449	0	
354.86	w	28172	276	
356.38	vw	28054	397	
357.40	vw	27971	480	
359.22	vw	27830	618	ν_s, α(C−C−C), 619 (R)
360.21	m	27754	695	ν_v, ϕ(C−C), 694 (R)
364.22	s	27447	1001	ν_p, ring, 1002 (R)
364.61	m	27419	1030	ν_b, β(C−H), 1029 (R)
365.77	ms	27334	1117	ν_q, X sens, 1116 (R)
366.40	w	27285	1164	ν_c, β(C−H), 1163 (R)
366.77	vw	27270	1191	ν_a, β(C−H)
371.20	m	26874	1575	ν_1, ν(C−C), 1575 (R)
372.21	s	26859	1590	ν_k, ν(C−C), 1590 (R)

[a] s = strong, m = medium, w = weak, v = very. [b] Frequency labels and descriptions from ref 15. (R) = observed in Raman spectrum at 77 K.

The HE system dominates the luminescences at 1.4 K. However, both systems are seen at both 77 and 1.4 K, with constant relative intensities at either temperature among multiple samples of the same compound. For example, although not evident from Figure 1, the LE system in $\{(Me_2PhP)AuBr\}_2$ is seen at 1.4 K with a peak intensity roughly a factor of 250 weaker than the HE emission. At room temperature, only relatively weak emission is seen. This is dominated by the LE system in the iodo dimer and the chloro trimer. The chloro and bromo dimers, however, show evidence of photodecomposition at room temperature, so that clean emission spectra could not be obtained. The energy and Franck−Condon envelope of the HE emission are very similar to those reported earlier for $(Ph_3P)AuX$ (X = Cl, Br).[9] The temperature dependences of the relative intensities of the HE and LE emissions are also similar to $(Ph_3P)AuX$. However, the energies and envelopes of the LE emissions differ significantly between the two groups of compounds.

At higher spectral resolution, the vibronic bands of the HE emission resolve into multiple emissive sites at ≤4.2 K with narrow line widths (≤5 cm^{-1}). The relative intensities of the sites vary significantly among different samples for some of the complexes. However, comparison of multiple spectra allowed a partial vibronic analysis for the most prominent site in each complex. These correspond in all cases to shallow traps (≤100 cm^{-1}; vide infra). As an example, the analysis of the HE emission of the chloro dimer is presented in Table 2 for the dominant trap at 1.4 K. The deduced vibrational frequencies, whose labels and assignments are based on the work of Whiffen,[15] are in good agreement with the observed Raman frequencies at 77 K. All of the prominent modes correspond to motions of the phenyl moiety. The modes around 1000 and

(11) Johnson, K. H. *Adv. Quantum Chem.* **1973**, *7*, 143. Slater, J. C. *Quantum Theory of Molecules and Solids*; McGraw-Hill: New York, 1974; Vol. 4. Connolly, J. W. D. In *Semiempirical Methods of Electronic Structure Calculation, Part A: Techniques*; Segal, G. A., Ed.; Plenum: New York, 1977; p 105. Case, D. A. *Annu. Rev. Phys. Chem.* **1982**, *33*, 151.
(12) The program was written by M. Cook and D. A. Case and obtained from QCPE. It was implemented locally on a MicroVAX 3100.
(13) Baenziger, N. C.; Bennett, W. E.; Soboroff, D. M. *Acta Crystallogr.* **1976**, *B32*, 962. Khan, M.; Oldham, C.; Tuck, D. G. *Can. J. Chem.* **1981**, *59*, 2714. Barron, P. F.; Engelhardt, L. M.; Healy, P. C.; Oddy, J.; White, A. H. *Aust. J. Chem.* **1987**, *40*, 1545. Einstein, F. W. B.; Restivo, R. *Acta Crystallogr.* **1975**, *B43*, 624.
(14) Weissbart, B.; Larson, L. J.; Olmstead, M. M.; Nash, C. P.; Tinti, D. S. *Inorg. Chem.* **1995**, *34*, 393.

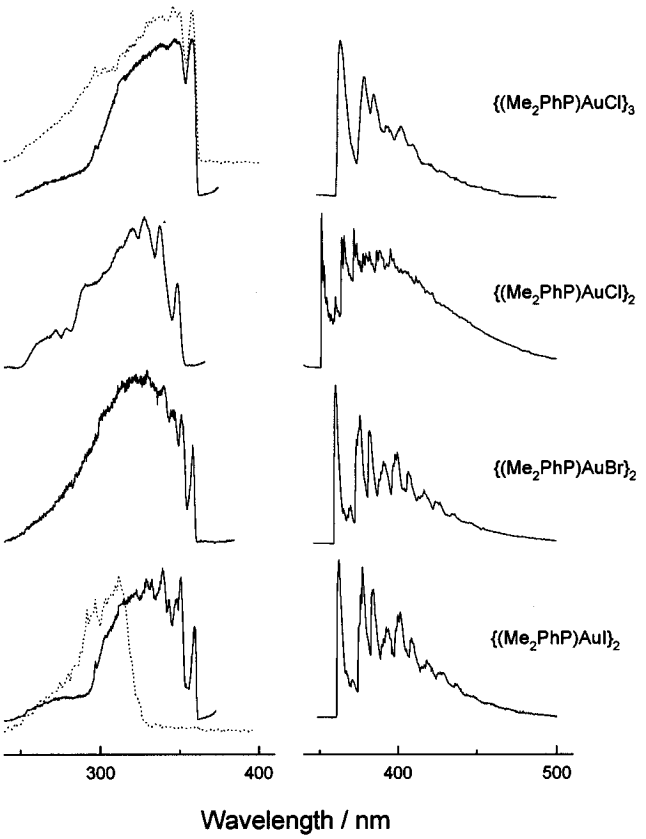

Figure 2. Comparison of the HE emission (right) and uncorrected photoexcitation (left) spectra of crystalline $\{(Me_2PhP)AuX\}_n$ at 1.4 K. The photoexcitation spectra are shown for monitoring the HE (solid lines) and LE (dotted lines) emissions.

1590 cm^{-1} form obvious progressions, as can be inferred from the lower resolution spectra given in Figure 2. The other complexes yield very similar results. The active vibrations parallel those seen in the HE emission of $(Ph_3P)AuX$.[9]

Figure 2 compares the HE emission spectra with uncorrected photoexcitation spctra for both the HE and LE emissions at 1.4 K. The excitation spectra for the HE emissions originate at ≈360 nm, overlapping the corresponding origin of the HE emission. The excitation spectrum for the LE emission in the chloro trimer shows the HE excitation spectrum plus a shoulder at ≈297 nm. For the iodo dimer, the LE excitation spectrum shows only a maximum at 309 nm with no significant signal from the HE system. The LE emission in the bromo dimer was too weak to record its excitation spectrum at 1.4 K. At 77 K the spectrum shows the excitation spectrum of the HE emission, as well as an unresolved shoulder to higher energy (≈300 nm). No excitation signal was detected for the LE emission at >360 nm for any of the complexes. Table 1 includes the low-resolution, photoexcitation origins and peaks for the HE and LE systems, respectively.

High-resolution absorption spectra were also obtained at 1.4 K for the dimers, using unoriented single crystals with thicknesses of ≈0.1 mm. These show a sharp (≤5 cm^{-1}) origin near 360 nm, followed to higher energy by only a few sharp lines and some broad bands. The absorption origins occur at 351.25, 359.66, and 360.51 nm for the chloro, bromo, and iodo dimers, respectively, and overlap (±5 cm^{-1}) the highest energy emission line of the corresponding complex. This indicates that the HE emission arises from unperturbed and slightly perturbed (shallow trapped) bulk molecules.

ODMR Spectra. The origin region of the HE emission and the intensity maximum of the LE emission were monitored at 1.4 K for ODMR signals in the frequency range 0.1−18 GHz for each crystalline complex. Signals were detected only while the HE emissions of $\{(Me_2PhP)AuCl\}_2$ and $\{(Me_2PhP)AuBr\}_2$ were monitored. As expected from the optical spectra, the ODMR spectra show signals from multiple sites. We focus on those ODMR signals which were assigned to particular sites. These signals were typically the most intense and involved the most intense and best resolved sites in the HE emission.

The signals for $\{(Me_2PhP)AuCl\}_2$ occur in the ranges 1.8−3.2 and 5.6−6.2 GHz and yield increases in the phosphorescence intensity at resonance. The strongest signal in each region, shown in Figure 3, is due to a site whose origin is at 352.57 nm (≈110 cm^{-1} trap). Other signals were associated with a higher energy site at 351.41 nm (≈10 cm^{-1} trap). The site at 352.57 nm has the largest emission intensity at 4.2 K, while the 351.41 nm site dominates the emission intensity at 1.4 K. The ODMR signals occur at 3.102 and 6.157 GHz for the 352.57 nm site and at 3.02 and 5.68 GHz for the 351.41 nm site.[16] No signals were detected at the sum or difference frequencies for either site. However, on the basis of earlier studies of the very similar HE emission of Ph_3PAuCl, which also shows ODMR signals in this range,[9] we assume that the unobserved third transition occurs at the difference frequency in each case. Table 3 summarizes the assigned frequencies and the deduced zero-field-splitting parameters, D and E.

The ODMR spectrum of the HE emission of $\{(Me_2PhP)AuBr\}_2$ differs significantly from that of $\{(Me_2PhP)AuCl\}_2$, contrary to the results found earlier for $(Ph_3P)AuBr$ and $(Ph_3P)AuCl$. The strongest signals for the HE emission of the bromo dimer are doublets near 2.7, 14.4, and 17.1 GHz, as shown in Figure 3. These are associated with an intense doublet (≈6 cm^{-1} splitting) at 359.78 nm (≤10 cm^{-1} traps). The ODMR doublet at intermediate frequency is a positive signal, whereas the other two are negative. The lowest frequency signal is complicated by multiple overlapping signals whose relative intensities depend strongly on sweep conditions. The frequencies and deduced splitting parameters are included in Table 3. Relative to the chloro dimer, $|E|$ is relatively unchanged at ≈0.05 cm^{-1}, but $|D|$ increases significantly from 0.15 to 0.5 cm^{-1}.

Kinetics. The kinetic parameters at 1.4 K of the HE emissions of the neat complexes were investigated by conventional emission decay measurements and by dynamic ODMR techniques at photostationary state.[17,18] The ODMR-derived data are limited to $\{(Me_2PhP)AuCl\}_2$ and $\{(Me_2PhP)AuBr\}_2$ and are only qualitative, since good signal-to-noice ratios could not be achieved. Assuming a relative ordering of the spin levels of $T_y > T_x > T_z$ and the absence of spin−lattice relaxation at 1.4 K, the ODMR data show $k_x \approx k_z > k_y$ for the total phosphorescence rates and $k_x^r \approx k_z^r > k_y^r$ for the radiative phosphorescence rates. These qualitative orderings agree with the quantitative ODMR results obtained for the HE emission in $(Ph_3P)AuCl$ and $(Ph_3P)AuBr$.[9] On the basis of the ODMR conclusions, the decay of the HE emission is predicted to appear biexponential in both $\{(Me_2PhP)AuCl\}_2$ and $\{(Me_2PhP)AuBr\}_2$ at 1.4 K. The observed decays indeed appear biexponential

(15) Whiffen, D. H. *J. Chem. Soc.* **1956**, 1350. Clark, R. H.; Flint, C. D.; Hempleman, A. J. *Spectrochim. Acta* **1987**, *43A*, 805.

(16) The signal at 3.02 GHz is a doublet, split by 7 MHz, which appears due to two sites whose origins overlap at 351.41 nm. The line shape of the 351.41 nm origin supports this contention. It is somewhat broader than that of other sites, with indication of an unresolved shoulder at lower energy.

(17) Winscom, C. J.; Maki, A. H. *Chem. Phys. Lett.* **1971**, *12*, 264.

(18) Shain, A. L.; Sharnoff, M. *J. Chem. Phys.* **1973**, *59*, 2335.

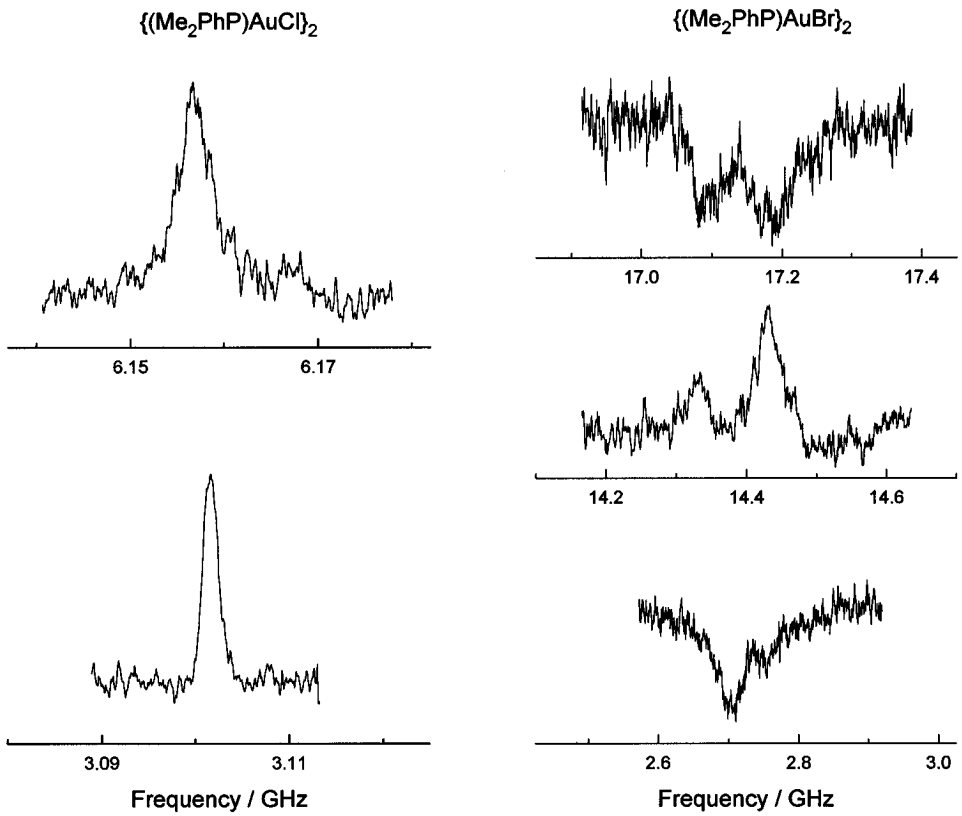

Figure 3. Example ODMR spectra monitoring the HE emission in crystalline $\{(Me_2PhP)AuCl\}_2$ and $\{(Me_2PhP)AuBr\}_2$ at 1.4 K.

Table 3. ODMR Frequencies and Zero-Field-Splitting Parameters for the HE Emission of Crystalline $\{(Me_2PhP)AuCl\}_2$ and $\{(Me_2PhP)AuBr\}_2$ at 1.4 K

				ZFS parameters/cm^{-1}	
site/nm	freq/GHz			$\|D\|$	$\|E\|$
		$\{(Me_2PhP)AuCl\}_2$			
351.38	5.68		3.02	0.138	0.050
352.57	6.157		3.102	0.1535	0.0517
		$\{(Me_2PhP)AuBr\}_2$			
359.78	17.181	14.427	2.744	0.527	0.0457
	17.091	14.323	2.771	0.523	0.0461

Table 4. Lifetimes of the HE and LE Emissions of $\{(Me_2PhP)AuX\}_n$ at 1.4 K for Pulsed Excitation at 337 nm

compound	site/nm	lifetime[a]
$\{(Me_2PhP)AuCl\}_2$	351.41	8.7 ms (0.9, 0.7[b])
		20 ms (0.1, 0.3[b])
	352.57	2.9 ms (0.6[c])
		13 ms (0.4[c])
$\{(Me_2PhP)AuBr\}_2$	359.78	200 μs (0.6)
		360 μs (0.4)
$\{(Me_2PhP)AuI\}_2$	360.5	$\leq$1 μs (0.95)
		14 μs (0.05)
$\{(Me_2PhP)AuCl\}_3$	360.5	10 μs (1.0)
	635	210 μs (1.0)

[a] Relative amplitudes in parentheses. [b] From shuttered decay. [c] From shuttered decay at 4.2 K.

with the parameters given in Table 4. The extracted lifetimes agree reasonably (±10%) with the ODMR derived data.[19]

For $\{(Me_2PhP)AuI\}_2$, the decay kinetics of neither the HE nor the LE band could be determined at 1.4 K with available instrumentation. The HE band decays too fast for our time resolution; only a limiting lifetime of $\leq$1 μs could be established. The LE band decays with a limiting lifetime of $\leq$1 ms from the shuttered decay. Its decay could not be measured at better time resolution with the N_2 laser since, as evident from Figure 2, it is not excited at 337 nm.

Both the HE and LE bands of the chloro trimer decay quickly at 1.4 K. The decays are exponential with lifetimes of 10 μs at 361 nm and 210 μs at 635 nm. The dependence of the LE lifetime on temperature between 1.4 and 30 K is given in Figure 4. This shows a sudden decrease with increasing temperature at about 5 K, indicating that an additional channel for depopulation of the LE excited state becomes thermally accessible around this temperature. The data are in good agreement with a model[20] involving three Boltzmann equilibrated levels, as shown by the solid line in Figure 4. The parameters, which were deduced using a least-squares algorithm with weights given by an assumed constant percent error in the lifetimes, are $1/k_1 = 211$, $1/k_2 = 43.4$, and $1/k_3 = 3.93$ μs with energy separations of $E_2 - E_1 = 12.5$ and $E_3 - E_1 = 26.0$ cm^{-1}. The energy levels were assumed nondegenerate. The lifetime at 77 K predicted by the parameters (13.4 μs) agrees well with the measured lifetime (11 μs).

Calculations. Figure 5 shows the orbital energy diagram that results from SCF−Xα−SW calculations on H_3PAuX and perpendicular $(H_3PAuX)_2$, with the orbitals numbering scheme discounting the core orbitals. In the monomers, the main consequence of varying the halogen occurs in the energy and description of the HOMO, which changes from $5a_1$ in H_3PAuCl to 4e in H_3PAuBr and H_3PAuI. The $5a_1$ orbital is Au centered with no significant halogen character, whereas the 4e orbital is dominated by halogen character. The partitioned charges are 48% Au-s and 40% Au-d for $5a_1$ and 65% Cl-p, 79% Br-p, and 87% I-p for 4e. Similar results occur from SCF−Xα−SW

(19) For example, the ODMR results for the 351.41 nm site of the chloro dimer yield $k_z^{-1} = 6.3$ ms, $k_x^{-1} = 7.7$ ms, and $k_y^{-1} = 20$ ms with $k_x^r \approx k_z^r > k_y^r$. Hence, the emission decay is expected to appear biexponential with lifetimes of ≈7 and 20 ms.

(20) Azumi, T.; O'Donnell, C. M.; McGlynn, S. P. *J. Chem. Phys.* **1966**, *45*, 2735. Harrigan, R. W.; Crosby, G. A. *J. Chem. Phys.* **1973**, *59*, 3468.

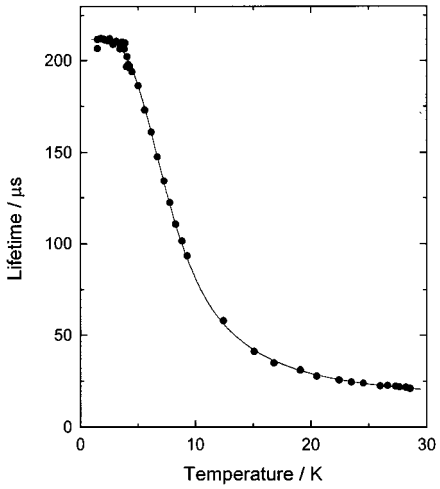

Figure 4. Lifetime of the LE band of crystalline $\{(Me_2PhP)AuCl\}_3$ between 1.4 and 30 K: points, experimental data; solid line, model calculation (see text).

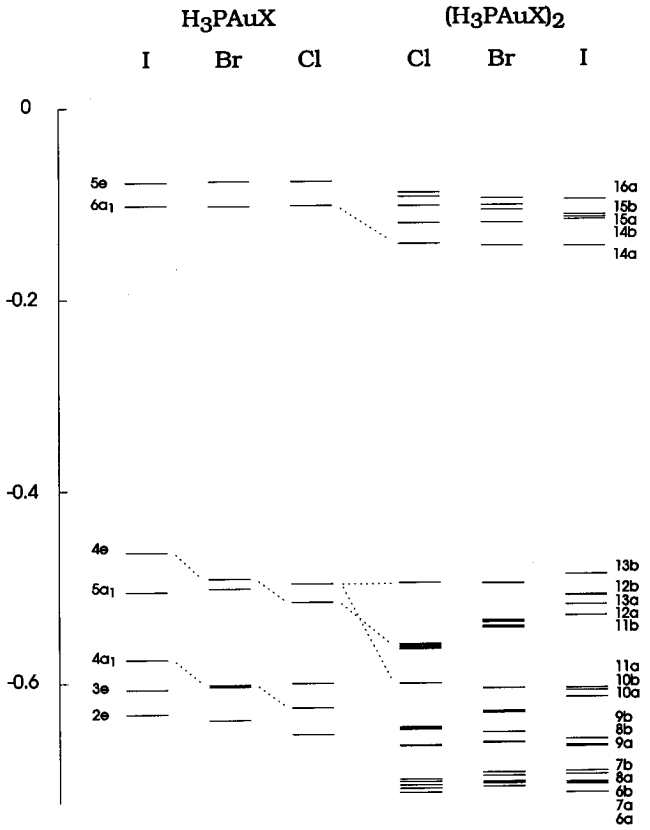

Figure 5. Orbital energies in rydbergs (1 Ry = 13.6 eV) from SCF−Xα−SW calculations for H_3PAuX in C_{3v} symmetry and $(H_3PAuX)_2$ in C_2 symmetry.

calculations in the HOMO of $XAuX^-$ with changing halogen.[21] In contrast, the LUMO of H_3PAuX remains $6a_1$ with a nearly constant charge distribution that is distributed over the Au (s+d, 30%) and halogen (s+d, 40%) centers. Hence, the LUMO−HOMO excitation is largely Au centered in H_3PAuCl, but it becomes a halogen-to-gold charge transfer in H_3PAuBr and H_3PAuI. The calculated gap is 5.36 eV in H_3PAuCl, 5.28 eV in H_3PAuBr, and 4.92 eV in H_3PAuI. The trend agrees with the abrupt red shift seen by Savas and Mason[22] of the lowest energy maximum in the absorption spectrum of $(R_3P)AuI$ (4.90 eV) relative to $(R_3P)AuBr$ (5.26 eV) and $(R_3P)AuCl$ (5.31 eV) for R = alkyl.

In the dimers, the symmetries of the HOMO (13b) and LUMO (14a) do not change with variation of the halogen, but their compositions behave as expected from the monomer results. Namely, in the HOMO the Au character decreases from 78% to 36% and the halogen-p character increases from 10% to 58% in going from Cl to I. No significant changes occur with variation of the halogen in the composition of the LUMO, whose charge distribution stays largest on Au (p, ≈32%). The LUMO−HOMO excitation can be classified roughly as a Au-based $\sigma(p) \leftarrow \sigma^*(s,d)$ transition, but its charge-transfer character increases from Cl to I. Its energy again shows a sudden, but smaller, red shift in the iodo complex, caused in the dimers by the destabilization of the HOMO that results from mixing with the lower-energy, mainly I-p orbitals (11b and 12b). The calculated gaps are 4.81, 4.79, and 4.65 eV in the Cl, Br, and I dimers, respectively. These show only moderate red shifts (0.3−0.6 eV) relative to the monomer.

Discussion

The HE emission observed from crystals of $\{(Me_2PhP)AuX\}_n$ is assigned as intraligand phosphorescence from a $^3\pi\pi^*$ state localized on the phenyl moiety of the phosphine ligand. This conclusion is based, in the present data, on the energy of the emission and its vibronic analysis, which shows only modes of the phenyl moiety. The strong similarities to the HE emission spectra of $(Ph_3P)AuX$, which have been similarly assigned, provide additional support.

Significant differences are seen, however, in certain properties of the $^3\pi\pi^*$ state between crystals of $\{(Me_2PhP)AuX\}_n$ and $(Ph_3P)AuX$. In the latter complexes, the zero-field splitting parameters, D and E, the phosphorescence lifetimes, k_i^{-1}, and the relative radiative rates, k_i^r, of the spin levels T_i ($i = x, y, z$) of the $^3\pi\pi^*$ state were relatively unchanged between the chloro and bromo complexes for several traps. The $(Ph_3P)AuX$ systems[9] have $|D| \approx 0.16-0.19$ cm^{-1}, $|E| \approx 0.03-0.04$ cm^{-1}, $k_x^{-1} \approx k_z^{-1} \approx 0.3$ ms, $k_y^{-1} \approx 1.4$ ms, $k_x^r \approx k_z^r \geq 40\%$, and $k_y^r \leq 10\%$ for an assumed relative ordering $T_y > T_x > T_z$. These same properties show large changes in $\{(Me_2PhP)AuX\}_n$ for different halogen ligands and for the same chloride ligand between the dimer and trimer oligomers. Only $\{(Me_2PhP)AuCl\}_2$ shows zero-field splittings similar to those seen in the monomeric triphenyl analog, although the phosphorescence lifetimes are longer for both of the studied traps in the chloro dimer than for the reported traps in the triphenyl complex.

The results for the $^3\pi\pi^*$ state in $(Ph_3P)AuX$ were interpreted in terms of spin−orbit interactions between a phenyl moiety and a gold center. The closest Ph···Au distances are similar in $(Ph_3P)AuX$ for the chloro and bromo complexes, and for inter- and intramolecular contacts, so that similar properties for the $^3\pi\pi^*$ state could result from either internal or external spin−orbit interaction with a Au center. However, the closest Ph··· Au, and Ph···X, distances are also very similar among the $(Ph_3P)AuX$ and $\{(Me_2PhP)AuX\}_n$ complexes, with the latter showing different, and strongly variable, properties of the $^3\pi\pi^*$ state. Hence, other considerations besides the Ph···Au or Ph···X distances must be important in moderating the spin−orbit interactions and in determining the detailed properties of the $^3\pi\pi^*$ state.

The explanation presumably involves the energy and/or detailed description of the perturbing state. If this state is mainly gold centered, then its enregy should remain relatively constant in the chloro and bromo $(Ph_3P)AuX$ monomers. In the $\{(Me_2-$

(21) Bowmaker, G. A.; Boyd, P. D. W.; Sorrenson, R. J. *J. Chem. Soc., Faraday Trans. 2* **1985**, *81*, 1627.
(22) Savas, M. M.; Mason, W. R. *Inorg. Chem.* **1987**, *26*, 301.

PhP)AuX}$_n$ oligomers, however, the energy of the lowest lying correlated state should be lower in the dimer and trimer, progressively. A smaller energy gap could lead to enhanced spin−orbit interaction with concomitant greater phosphorescence rates and zero-field splittings for the $^3\pi\pi^*$ state. The largely Au-based σ(p) ← σ^*(s,d) excitation likely provides the perturbing states. Its singlet state is observed at ≈4.3 eV (vide infra), which is ≤1.0 eV above the observed $^3\pi\pi^*$ state. The calculations indicate that the interaction could be sensitive to the halogen, in terms of both the energy and the composition of the perturbing state. Interestingly, the major phosphorescence rates, and available splitting parameters, increase approximately as the Au···Au separations (I ≈ Cl(trimer) < Br < Cl(dimer))[10] decrease.

The available data for the LE emissions in {(Me_2PhP)AuX}$_n$ are more limited, and their assignment is consequently less definitive. The emission is clearly different from the LE emission seen in the monomeric (Ph_3P)AuX complexes. Its energy is lower, its lifetime is shorter, and it shows no vibronic structure. The LE emissions in both groups of compounds originate from triplet states, but the zero-field splittings are grossly different. The LE emissions in (Ph_3E)AuX have very small zero-field splittings ($D \approx 0.09$ cm^{-1}).[9] The dependence of the LE lifetime on temperature in the chloro trimer points to a triplet multiplicity with very large zero-field splittings ($|D| = 20$ and $|E| = 6$ cm^{-1}). We assume that the LE emissions in the bromo and iodo dimers also represent phosphorescence from a triplet state with large zero-field splittings. Large zero-field splittings require large spin−orbit interactions, necessitating large amplitudes on heavy-atom centers in the excited or perturbing state. The SCF−Xα−SW calculations presented herein for (H_3PAuX)$_2$, and similar SCF−Xα−SW calculations by King et al.[2] for [Au($H_2PCH_2PH_2$)]$_2^{2+}$ and extended Hückel calculations by Assefa et al.[4a] for {(TPA)AuCl}$_2$ (TPA = 1,3,5-triaza-7-phosphaadamantane), indicate that the lowest energy, Au-based excitation involves the $\sigma \leftarrow \sigma^*$ transition. The same transition, red-shifted by the additional interactions, should be the lowest energy, Au-based excitation in a linear trinuclear Au(I) complex. King et al.[2] have assigned the emission of various supported binuclear Au(I) complexes with emission maxima around ≈500 nm to phosphorescence due to the $\sigma \leftarrow \sigma^*$ excitation. Assefa et al.[4] make the same assignment for the 590−680 nm emissions in unsupported binuclear Au(I) complexes.

The present results show that the HE emission is associated with bulk and shallow trapped {(Me_2PhP)AuX}$_n$ molecules. This is evidenced by the agreement between the absorption and the highest energy emission origins and among the vibrational frequencies from the Raman and HE emission spectra. No corresponding evidence exists for the broad LE emission. The two emissions have different photoexcitation spectra, but the solution absorption spectra show bands in the regions of both photoexcitation spectra. The HE photoexcitation spectrum corresponds to a weak absorption reported for solutions of (Ph_3P)AuX,[9] while an absorption peaking near the wavelength of the LE photoexcitation band is seen for solutions of (Me_2PhP)AuI with a quadratic dependence of its absorbance on (monomer) concentration.[10] Hence, the absorption data allow for the two emissions to arise from a common {(Me_2PhP)AuX}$_n$ center. The localizations of the excited states on the separated phenyl and metal moieties, along with possible geometry changes in the excited states, also permit slow energy relaxation through unfavorable Franck−Condon factors. Such considerations *might* explain the different photoexcitation spectra and thermally nonequilibrated phosphorescences from two triplet states on a common {(Me_2PhP)AuX}$_n$ center. However, this is not expected, particularly in a neat solid, for the large energy gap between the same multiplicity, triplet excited states of the HE and LE emissions.

The calculated HOMO−LUMO gaps for H_3PAuX are 4.9−5.4 eV, in good agreement with the lowest energy maxima reported by Savas and Mason[21] in the solution absorption spectra of the corresponding alkylphosphine complexes. The calculated gaps for (H_3PAuX)$_2$ are 4.6−4.8 eV. These can be compared with the solution absorption spectra and assignments given by Jaw et al.[23] for the supported binuclear complexes [Au_2(dmpm)$_2$]$^{2+}$ (dmpm = bis(dimethylphosphino)methane), [Au_2(dmpe)$_2$]$^{2+}$ (dmpe = bis(dimethylphosphino)ethane), and [Au_2(dmpm)$_3$]$^{2+}$. The Au···Au separation in crystals of these complexes range from 2.87 to 3.05 Å.[23] The singlet state arising from the $\sigma \leftarrow \sigma^*$ excitation was assigned to an intense band at 4.56−4.85 eV, in good agreement with the calculated HOMO−LUMO gaps, while a weaker band at 3.82−4.00 eV was assigned to a spin−orbit component of the corresponding triplet state. These two bands are the lowest energy bands seen in the absorption spectra.

The LE emissions at 630−730 nm in {(Me_2PhP)AuX}$_n$, with Au···Au separations of 3.09−3.23 Å,[10] show photoexcitation maxima at ≈4.3 eV. Very similar energies are seen for the photoexcitation maxima associated with the 500 nm emission of [Au_2(dppm)$_2$]$^{2+}$ (dppm = bis(diphenylphosphino)methane, 4.4 eV, Au···Au = 2.96 Å)[2] and with the 590−680 nm emissions of {(TPA)AuX}$_2$ and protonated products (X = Cl, Br, I, 3.8−4.3 eV, Au···Au = 2.92−3.32 Å).[4] The energies of the excitation maxima, for the similar Au···Au separations, are consistent with an assignment of the band to the singlet state of the $\sigma \leftarrow \sigma^*$ transition in the three groups of complexes. This prompts the assignment of the (LE) emissions in the three groups of complexes to the corresponding triplet state, yielding triplet energies of 1.7−2.5 eV. These show an ≈2 eV shift to lower energy than suggested by Jaw et al.[23] Part of the disagreement, however, could reflect a Stokes shift between the absorption and emission maxima, caused by the anticipated shortening of the Au···Au separation in the excited triplet state. A large splitting between the singlet and triplet states of the $\sigma \leftarrow \sigma^*$ transition, as discussed by Assefa et al.,[4] agrees roughly with the splitting between the ^{1}D and ^{3}D terms for the free Au(I) ion. The absence of a simple correlation between the energies of the states derived from the $\sigma \leftarrow \sigma^*$ transition and the Au···Au distances has been previously noted for dissimilar systems,[2] but such correlations are predicted and have been reported when no other variables are involved.[4]

Although the calculations indicate that changes occur in the energy and composition of the $\sigma \leftarrow \sigma^*$ excitation for variation of the halogen ligand, the experimental results do not substantiate the predictions. For example, the calculated excitation energies are very similar in the chloro and bromo dimers with a red shift (1100 cm^{-1}) in the iodo dimer. The experimental results for the LE emission show a blue shift (1600 cm^{-1}) in the iodo dimer relative to the bromo dimer. The Au···Au distances are very similar in the iodo and bromo dimers (smaller in the iodo dimer by only 0.015 Å[10]), suggesting that other considerations are important in determining the energy of the LE emission. Of course, various interactions that affect state energies are neglected in the calculations, as witnessed by the large singlet−triplet splitting.

(23) Jaw, H.-R. C.; Savas, M. M.; Rogers, R. D.; Mason, W. R. *Inorg. Chem.* **1989**, *28*, 1028. Jaw, H.-R. C.; Savas, M. M.; Mason, W. R. *Inorg. Chem.* **1989**, *28*, 4366.

The dimeric complexes $\{(TPA)AuX\}_2$, which do not contain phenyl moieties, also show both a structured HE and an unstructured LE emission from two thermally nonequilibrated excited states in neat crystals.[4] The energy, lack of vibronic structure, lifetime in the microsecond range, and photoexcitation maximum of the LE emission are very similar to those seen in $\{(Me_2PhP)AuX\}_n$, and, as already noted, the excited state involved has been assigned similarly to the triplet state associated with the Au-based $\sigma \leftarrow \sigma^*$ excitation. The HE emissions in the two groups of complexes show large differences. In $\{(TPA)AuX\}_2$, the origin of the HE emission is red-shifted by $\approx$4500 cm^{-1} to $\approx$420 nm, its vibronic structure shows mainly lower frequency modes, and the lifetime is much shorter (in the nanosecond range). This HE emission has been assigned as fluorescence from a singlet state due to a halide-to-metal charge transfer excitation (^{1}XMCT). No evidence of this fluorescence emission is seen in $\{(Me_2PhP)AuX\}_n$. If this ^{1}XMCT state remains near the same energy, then it appears that the phenyl-localized $^3\pi\pi^*$ state acts as a trap which stops population of the lower lying ^{1}XMCT state.

Conclusions

Crystals of $\{(Me_2PhP)AuX\}_n$ with X = Cl, Br, and I show emission from two excited states at low temperatures. The HE emission, which originates at $\approx$360 nm, is due to intraligand phosphorescence from a phenyl-localized $^3\pi\pi^*$ state. The bulk of its emission intensity arises from slightly perturbed (shallow trapped) molecules of $\{(Me_2PhP)AuX\}_n$. The HE emission strongly resembles an emission seen in crystals of $(Ph_3P)AuX$, which has been similarly assigned. The zero-field splittings and phosphorescence rates of the $^3\pi\pi^*$ state in $\{(Me_2PhP)AuX\}_n$ vary strongly for different halogens, contrary to the behavior in $(Ph_3P)AuX$.

The LE emission, which peaks at 630−730 nm, is also phosphorescence. Its excited state has a large amplitude on the gold center, on the basis of the large zero-field splittings and short lifetimes, and it is assigned a gold-based $\sigma \leftarrow \sigma^*$ parentage. The corresponding singlet state occurs at 290−310 nm. The results are not inconsistent with both the HE and LE emissions arising from a common $[(Me_2PhP)AuX]_n$ center. However, assigning the two emissions to different $\{(Me_2PhP)AuX\}_n$ traps eliminates the problems associated with dual phosphorescences from states with a large energy difference.

Acknowledgment. We thank the National Science Foundation for support (Grants CHE 9022909 and CHE 9321257) and Dr. Marilyn M. Olmstead for calculations related to the crystal structures.

IC951100M